Astron. Astrophys. 229, 216–223 (1990)

ASTRONOMY AND ASTROPHYSICS

Computation of electron beam parameters for solar type III and J bursts

A. Hillaris [1], C.E. Alissandrakis [1], C. Caroubalos [2], and J.-L. Bougeret [3]

[1] Section of Astrophysics, Astronomy and Mechanics, Department of Physics, University of Athens, GR-15783 Athens, Greece
[2] Laboratory of Electronics, Department of Physics, University of Athens, GR-15873 Athens, Greece
[3] Observatoire de Paris, Department de Recherche Spatiale, CNRS UA 264, F-92195 Meudon Cedex, France

Received June 26, accepted July 18, 1989

Abstract. The dynamic evolution of mildly relativistic electrons (10–100 keV) propagating outwards in the solar corona following open or closed magnetic lines is studied using the drift approximation. Wave-particle interactions are neglected, since the beam-plasma system is considered as almost decoupled in the range of parameters used in this model. The results of this simulation are used for the computation of observable quantities and the analysis of dynamic spectra of isolated type III or J bursts, obtained with the Digital Multichannel Radio Spectrograph of the Space Research Laboratory of Paris, Meudon. The initial velocity dispersion of the exciter and the coronal scale height are thus determined. The implications of the results on the emission processes are discussed.

Key words: Sun: type III bursts: J-bursts – Sun: beam-plasma interaction

1. Introduction

Type III radio bursts are the observable manifestation of the propagation of beams of mildly relativistic electrons along open magnetic field lines in the solar corona (Wild and McCready, 1950), while U bursts evidence their propagation in closed magnetic field lines. In the case of type III bursts the radio emission drifts rapidly towards lower frequencies at a rate which is almost proportional to the frequency, whereas in the case of U bursts the emission drifts initially towards lower frequencies, but after reaching a turnover point (at a minimum frequency which corresponds to the maximum altitude of the loop) the sense of the drift reverses, thus giving the appearance of an inverted letter U in the dynamic spectrum (Wild, 1970).

Some U bursts have a very faint descending branch and appear as an inverted letter J on the dynamic spectrum recordings (Fokker, 1969). Many of the dynamic spectra of the so called J bursts resemble strongly those of type III events, so that a thorough examination is needed to distinguish between them. A fourth member of the type III family was discovered recently, the so called N bursts (Caroubalos et al., 1987), the dynamic spectra of which provide evidence for reflection of the beam at the other end of the loop.

The time profile of a type III, U, J or N burst at a given frequency is believed to represent the passage of the electron beam through that frequency level. The burst duration is believed to be related to the length of the exciter rather than the response of the medium and was found to increase with time, which indicates an increase of the duration with the distance traversed by the beam (Poquerusse et al., 1984).

In a previous article (Hillaris et al., 1988, hereafter referred to as Paper I) we considered the propagation of a mildly relativistic electron beam in a closed coronal loop and we showed that non-linear effects result in an almost free streaming behaviour; thus we were able to reproduce the qualitative characteristics of the dynamic spectra of N bursts. In this paper we extend the free streaming computations and we consider the cases of type III and J bursts. The results of our computations are compared with observations of isolated events and provide diagnostics of the initial beam velocity dispersion, the coronal scale height and the relation between the beam density and the intensity of the electromagnetic radiation. Seven events observed with the Digital Multichannel Radiospectrograph of the Space Research Laboratory of the Observatory of Paris, Meudon (Dumas et al., 1982) have been analysed.

2. Free-streaming evolution of a superthermal electron population

The Radiospectrograph observations give the intensity of the electromagnetic radiation as a function of frequency and time. Our computations have been done in two steps: in the first step we computed the instantaneous density of the electron beam as a function of time and distance from its source, while in the second we associated this density to the level of the electromagnetic emission.

The interaction of a superthermal electron population with the plasma under solar coronal conditions has been treated in detail in Paper I, thus only a brief outline will be given here. In the linear regime the beam plasma system is unstable. Plasma waves, W_k, with phase velocities $v_{ph} = \omega_e/k \leqq v_b$ will grow at a rate γ_l where:

$$\gamma_l = (N_b/N)\ (v_b/\Delta v_b)^2\ \omega_e\ . \qquad (1)$$

In this expression N is the density of the ambient plasma and N_b is the density of the beam with an average velocity v_b and a velocity dispersion Δv_b.

The resonant Langmuir wave will diffuse the beam particles in velocity space, forming a quasi-plateau for the beam distribution (Zheleznyakov and Zaitsev, 1970). The quasilinear evolution of

Send offprint requests to: A. Hillaris

the beam interaction with the ambient plasma is described by the equations:

$$\left(\frac{\partial}{\partial t} + v\frac{\partial}{\partial s}\right) f_b = \frac{\partial}{\partial v} D \frac{\partial}{\partial v} f_b - \nu_c f_b \,, \tag{2a}$$

$$\partial W_k/\partial t = \gamma_l W_k \,, \tag{2b}$$

where $D = (4\pi e/m)^2\, \omega_e/v$ (see for example Ryutov and Sagdeev, 1970), W_k is the spectral energy density of the Langmuir waves, and ν_c a Krook collision term (Bhatnagar et al., 1954).

It has been shown (Papadopoulos, 1975) that Langmuir ion acoustic wave coupling via the ponderomotive force can efficiently transfer the energy of the resonant Langmuir wave into lower phase velocities. In addition the growing ion acoustic modes can also scatter Langmuir waves out of resonance with the beam; when such processes take place in a time interval less than the characteristic time for the generation of the beam-resonant waves, the level of wave energy density W_k remains low at all times and Eq. (2a) can be replaced by the free-streaming equation with a collision term:

$$\left(\frac{\partial}{\partial t} + v\frac{\partial}{\partial s}\right) f_b = -\nu_c f_b \,. \tag{3}$$

The phenomenological term ν_c for the effective collision frequency includes both Coulomb collisions and collisions on ion acoustic density fluctuations. Hence ν_c is written as the sum of the terms $\nu_c = \nu_{cc} + \nu_{ci}$ where:

$$\nu_{cc} = 4\pi\, Ne^4\, L\,(\mu_{ie}^{-2} + \mu_{ee}^{-2})/v^3 \tag{4a}$$

(see for example Ishimaru, 1986); μ_{ie}, μ_{ee} are the reduced masses for electron-ion and electron-electron collisions respectively and

$$\nu_{ci} = [k_s \lambda_d\, W_3/N\, kT_e]\; (v_e/v)^3\, \omega_e \tag{4b}$$

(Papadopoulos, 1977) where k_s is a characteristic wave number of ion-acoustic waves, λ_d the Debye length and we take $k_s \lambda_d = 2\pi/10$ (Vlahos and Rowland, 1984), W_3 the ion acoustic wave energy density, v_e the thermal velocity of the ambient plasma.

For the purposes of this computation we have used a one dimensional model with homogeneous magnetic field; we assumed that 10^{13} particles, with a velocity spread δv (in the range 0.2 to 0.7 c), are injected in an open magnetic flux tube within a time interval t_{inj} (ranging from 0.10 to 0.70 s). The injected distribution is assumed to have the following form:

$$f_0\,(v, s, t) = [N_{b0}/(t_{inj}\, \delta v\, \sqrt{\pi})]\, \exp(-v^2/\delta v^2)\; T\,(t)\; \delta\,(s) \,, \tag{5}$$

where N_{b0} is the initial density of the beam and $T\,(t)$ models the injection rate as a function of time. For simplicity we assumed that it has the form of a square pulse of duration t_{inj}. We have assumed that the injection region is much smaller than the distance traversed by the beam, hence the delta function in Eq. (5).

The total collision frequency ν_c was calculated assuming $T_e \approx 10^6$ K, $N_e \approx 10^9\,\mathrm{cm}^{-3}$ (this corresponds to the average density in the frequency range of the Radiospectrograph, 470–150 MHz); we further assumed that $W_3/NkT_e \approx 10^{-6}$ (Paper I), thus for ν_c we used values in the range of 1 to 1.6 $10^{29}/v^3\,\mathrm{s}^{-1}$.

Equation (3) is easily integrated giving:

$$f_b\,(v, s, t) = \int_0^t \exp\,[-\nu_c\,(t-t')]\; f_0\,(v, s - v\,(t-t'),\, t')\; \mathrm{d}t' \tag{6}$$

(see also Raoult et al., 1990). The instantaneous beam density is calculated by integration of (6) over the velocity:

$$N_b\,(s, t) = \int_0^\infty f_b\,(v, s, t)\; \mathrm{d}v \,. \tag{7}$$

In Paper I, following Vlahos and Rowland (1984), we have used the notation W_1, W_2, W_3 for the normalised energy density of the beam resonant Langmuir wave, the out of resonance electrostatic wave and the ion sound respectively. The dependence of W_1, W_2, W_3 on the beam to ambient plasma density ratio N_b/N was found to be, $W_1 \propto (N_b/N)^2$, $W_3 \propto (N_b/N)$, while W_2 was much smaller than W_1 and virtually independent from N_b/N.

After Papadopoulos and Freud (1979), we may assume the following mechanisms for the conversion of the electrostatic modes into electromagnetic radiation either near the fundamental or the harmonic of the local plasma frequency.

(a) Scattering of Langmuir waves (W_1) on the ion acoustic wave W_3. The volume emisivity $P\,(\omega_e)$ is proportional to the product $W_1\, W_3$ (Emission at the fundamental).

(b) Scattering of Langmuir waves on the polarization clouds of the ions, which also give emission at the fundamental with a volume emissivity $P'\,(\omega_e)$ proportional to W_1 (see also Smith and Davis, 1975).

(c) Coalescence of Langmuir waves with opposite phase velocities. This can be done by the two counterstreaming "components" of the non resonant wave W_2, (let them be W_{2+} and W_{2-}) giving harmonic radiation with a volume emisivity $P''\,(2\omega_e)$ proportional to $W_{2+}\, W_{2-}$.

Hence we may assume a power law dependence of the radiation intensity on the beam to ambient plasma density ratio:

$$W_{em} \propto (N_b/N)^a \,. \tag{8}$$

In situ measurements made by Fitzenreiter et al., (1976) indicate a power law dependence of the flux of radio emission on the beam electron flux ($J_r \propto J_e^a$ where J_r, J_e are the measured radio and electron flux respectively). After analysing ten solar wind type III bursts observed by IMP-6 and Apollo 16 at 1 AU, they found values of the power law index, a, within the range 0.80–1.37 for five bursts and within the range 2.21–2.63 for three others. For the remaining two bursts they reported a transition from 0.84 and 0.92 to 2.38 and 2.54 respectively. These results were confirmed by the solution of the non-linear beam-plasma equations for a fully evolved exciter (Goldstein et al., 1979; Papadopoulos, 1980) and for typical solar wind parameters. More recent in situ measurements at 1 AU by ISEE-3 (Lin, 1985) revealed, in addition to the energetic electrons and radio emission, highly impulsive plasma oscilations which were clearly associated with the electron and radio fluxes observed in interplanetary type III bursts. The spiky appearance of the plasma oscilations is probably due to the interaction of the growing Langmuir waves with ion acoustic density fluctuations (see Paper I, also Vlahos and Rowland, 1984).

The discussion above outlines the difficulties inherent in the attempt to correlate instant beam density to the radio emission of the resulting burst. Density irregularities and ion acoustic waves already present in the corona may significantly affect, not only the stabilization and evolution of the streaming beam, but also the decay processes of the electrostatic and ion acoustic modes into transverse waves. Hence the index a is treated as free parameter in the calculations and its value will be determined by comparison with our observations. These values can provide information about the emission processes in the type III and J events.

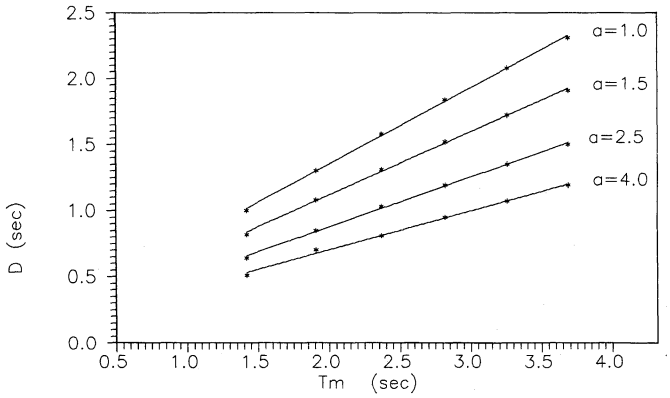

Fig. 1. Half power duration of the electromagnetic emission as a function of the time of maximum and the power law index a, for a streaming beam with velocity dispersion $0.3\,c$, injection duration of 0.1 s and effective collision frequency $1.3\ 10^{29}/v^3\,s^{-1}$

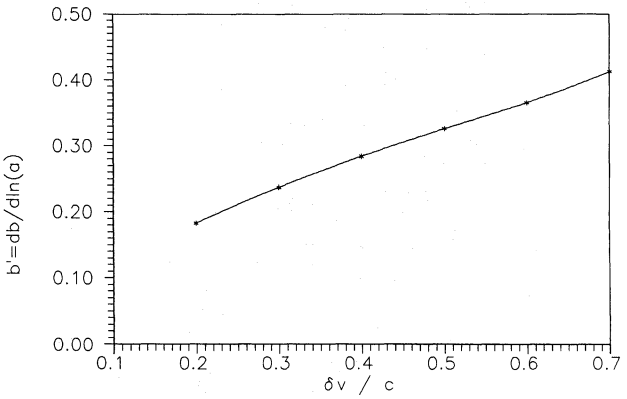

Fig. 3. The "form factor" b' (derivative of b with respect to the power law index) as a function of the velocity dispersion of the exciter

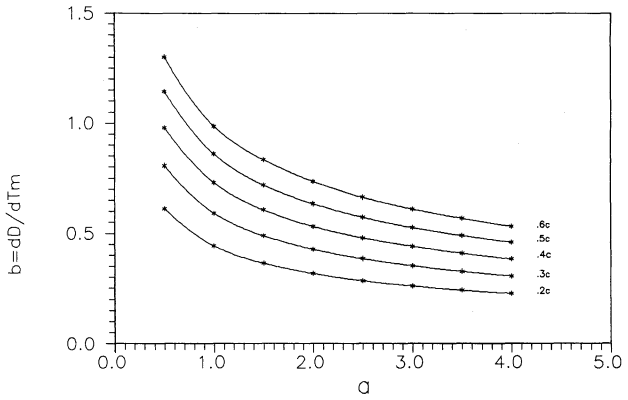

Fig. 2. The "form factor" b (derivative of the duration with respect to time) as a function of the assumed power law index a and the velocity dispersion δv of the exciter; the curves have been averaged over collision frequencies (1–1.6 $10^{29}/v^3\,s^{-1}$) and injection durations (0.1–0.7 s)

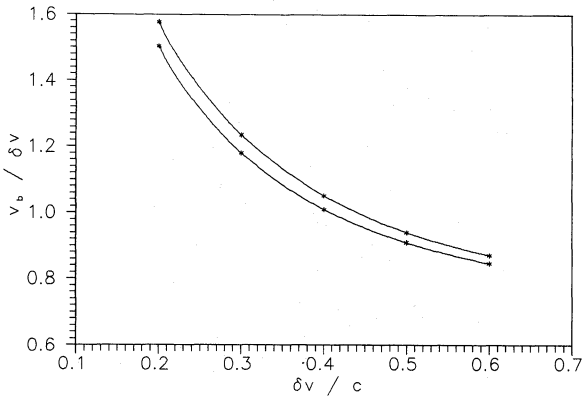

Fig. 4. The apparent drift velocity as a function of the velocity dispersion of the exciter. The upper curve corresponds to collision frequency of $1.6\ 10^{29}/v^3\,s^{-1}$, the lower to $10^{29}/v^3\,s^{-1}$

3. Results of the computations

Using the free streaming approximation we computed time profiles of the intensity of the emission at given distances traversed by the beam from the injection point. The parameters used in our simulations were the power law index, a, the initial velocity dispersion of the exciter, δv, the injection duration, t_{inj}, and the effective collision frequency, ν_c.

The computed intensity-time profiles at a given distance from the injection region (which corresponds to a given frequency) resemble strongly to the observed intensity-time profiles of type III or J bursts (see Fig. 5a, Paper I). The decay part is almost exponential, while the rising part is slightly steeper than the decaying. This intensity-time profile is a well known characteristic of type III bursts reported by many investigators in various frequency ranges (see for example Poquerusse, 1977, in the range 171–167 MHz; Barrow and Achong, 1975, in the range 18–36 MHz; Weber, 1978, in the 3 MHz to 55 kHz range). In this section we will derive observable quantities from our simulations which will be used for comparisons with the observations.

From the computed time profiles we calculated the half power duration, D, of the electromagnetic emission, as a function of the time interval between the maximum of the emission and the injection time, T_m, and the parameters of the model. Our results show that the half power duration has an almost linear dependence on the time of maximum (Fig. 1). Moreover, the rate of change of the duration with time of maximum defines a "form factor" b, $(= dD/dT_m)$, which depends primarily on the index a and the velocity spread δv of the exciter; sine in the range of ν_c and t_{inj} used the results of the simulation do not vary more than 10% we used the average over these two parameters which were thus eliminated.

The dependence of b on δv and a is shown in Fig. 2. We note that, for a given density-time profile, a small value of a will give a wide intensity profile and hence the decrease of b with a. The increase b with the initial velocity dispersion of the beam is a consequence of the faster broadening of the beam.

The dependence of b on the logarithm of a is, to a very good approximation, linear. Thus each curve of Fig. 2 can be described by the parameter $b' = -\,db/d\ln(a)$ which now depends only on δv (Fig. 3). Our computations show further that the time of maximum is proportional to the distance traversed by the beam, i.e. the apparent (drift) velocity of the electron cloud, v_b, is constant with time; its value depends on the initial velocity spread δv of the electron population. The results are shown in Fig. 4. The two curves correspond to the extreme values of the collision frequency

used; here again the effect of the collision frequency is small. For $\delta v < 0.4\,c$ ($120\ 10^3$ km s^{-1}) the drift velocity of the beam is greater than the initial velocity dispersion, because the collision term ν_c ($\propto v^{-3}$) is much more efficient in the low velocity regime and as a result only the fastest electrons from the initial population survive. For high values of δv this effect saturates and the drift velocity approaches 80% of the velocity dispersion.

4. Observations and data reduction

The observations were made with the Nançay Multichannel Radiospectrograph in the 470–150 MHz range (Dumas et al., 1982). The output of 120 independent frequency channels is recorded on photographic film; this output is almost proportional to the logarithm of the antenna temperature, thus increasing the dynamic range of the instrument. Thirty two channels are digitized at a rate of 10 samples s^{-1} and recorded on magnetic tape. Each channel has a bandwidth of 1 MHz at 3 dB and their frequencies are logarithmically spaced.

The calibration is performed twice a day in the following way: The receiver is disconnected from the antenna and connected to a noise source of known temperature. Moreover, in order to correct for non linearities of the almost logarithmic I.F. stage of the receiver, we record its response to a noise source with intensity varying in steps of 1 dB. This method of calibration extends the dynamic range of the instrument to about 60 dB and is particularly useful at the low intensity levels.

It is well known that events of the type III family generally occur in groups and, more often than not, the emission of several individual bursts is superimposed on the dynamic spectrum. Such groups are not appropriate for the determination of the parameters describing the beam propagation, thus a careful selection of isolated events was made by visual inspection of the films. We found only 12 cases of apparently isolated events for which digitized data were available, in the interval of May 1980 to May 1983. Further examination of the digital data reduced the number of usable isolated events to 7. Their dynamic spectra, reconstructed from the calibrated digital data, are shown in Fig. 5; the dates and times of observation are listed in Table 1. Two of the seven selected events were type III (those of November 22 and 23, 1982) while the other five were J bursts.

The bursts were associated with Hα activity reported in the Solar Geophysical Data Bulletin; all time intervals were corrected for geometric effects by multiplying with the factor:

$$K = (1 - \cos\varphi \cos\lambda\, v_b/c)\,, \tag{9}$$

where φ is the latitude and λ the longitude of the associated active region. This approach assumes a radial propagation path; no correction was made for wave propagation effects.

In the previous section we derived relations between the beam parameters and observable quantities such as the drift velocity of the beam and the form factors b and b' which are related to the evolution of the half power duration of the electromagnetic emission. The logarithmic frequency drift rate is easily measured in the dynamic spectra and it is related to the drift velocity of the beam through the scale height along the beam trajectory; knowledge of the scale height would give the drift velocity and subsequently the velocity dispersion could be determined from Fig. 4. However the trajectory of the beam may be inclined with respect to the vertical and moreover the temperature of the coronal plasma along the path of the beam is not well known; thus a reliable estimate of the scale height cannot be made.

The half maximum duration D of the electromagnetic intensity profile is directly measurable and so is its derivative with respect to the time of maximum i.e. the form factor b. The measurement of the form factor b', requires a more elaborate treatment: Let a_0 be the true value of a; suppose now that a takes the value of $\xi\, a_0$. The same density time profile would give a different intensity profile and hence a different half power duration. Due to the assumed power law dependence of the intensity on the beam density, that duration would be equal to the duration of the observed profile measured at the level $I = I_{max}\, 2^{-1/\xi}$, where I_{max} is the peak intensity. Thus the duration as well as b can be computed as a function of ξ. It is easy to show that the derivative of b with respect to $\ln\xi$ is the same as its derivative with respect to $\ln a$, since a_0 is a constant.

We found that, for a given value of ξ, the observed duration is proportional to the time of maximum (see examples in Figs. 6a and 7a) in good agreement with our theoretical results of Sect. 3. Moreover, the paramerer b has a linear dependence on the logarithm of ξ, again in good agreement with the theory (Figs. 6b and 7b). Thus for each event a unique value of the parameter b' is obtained, from which the velocity dispersion of the exciter can be determined (Fig. 3). Once δv and b are known the actual value of a_0 can be computed from Fig. 2. The results are shown in Table 1.

The velocity dispersion of the exciter was in the range of 0.13 to $0.60\,c$, which implies energies of the order 3–100 Kev. The power law index was in the range of 1.3 to 2.8 which is consistent with the results of Fitzenreiter et al., 1976 for the Solar wind type III events. Mechanisms (a) and (b) (cf. Sect. 2) for radiation at the fundamental predict that the electromagnetic emission flux is proportional to the cube and the square of the beam to background density ratio respectively; the values deduced for the power law index indicate that both mechanisms may be responsible for the radio emission. It is difficult to compare our results with the prediction of the third mechanism, since the rate equations used do not distinguish between W_{2+}, and W_{2-}, but give only the total energy density, W_2, of the non-resonant Langmuir wave.

Using the computed values of the velocity dispersion, δv, together with the results shown in Fig. 3, we computed the drift velocity of the beam (Table 1). The results are in the range of 0.24 to $0.52\,c$, which is consistent with the values determined by positional measurements made in the 2.8–0.7 MHz range, by Fainberg and Stone (1970) (see also Wild and Smerd, 1972) as well as with the in situ measurements of ISEE 3 (Lin et al., 1981) and IMP-6 (Alvarez et al., 1975). The drift velocity of the beam and the observed logarithmic frequency drift give the density scale height of the corona, H, along the beam trajectory. The two quantities are related through:

$$H = -0.5\, v_b\, (\mathrm{d}\ln f/\mathrm{d}T_m)^{-1}\,. \tag{10}$$

The results are also given in Table 1. The density scale height of the two type III bursts was 78 and 74 10^3 km; this corresponds to a temperature of 1.5 10^6 K, which is approximately the temperature of the solar corona. The scale height for the J bursts was in the range of 112 to 325 10^3 km; assuming that the increased scale height is due to the inclination of the beam trajectory with respect to the vertical and a coronal temperature of 2 10^6 K, these values imply inclinations of 25 to 70°. Alternatively, the higher values of the scale height for the J bursts could be attributed, at least in part, to the increased temperature of closed magnetic loops.

As a self consistency test of our procedure we computed for each event an average observed time profile, using a similarity property of type III bursts. For this purpose the time profiles at different frequencies were scaled in intensity, scaled and shifted in time and subsequently were superposed to give a single time

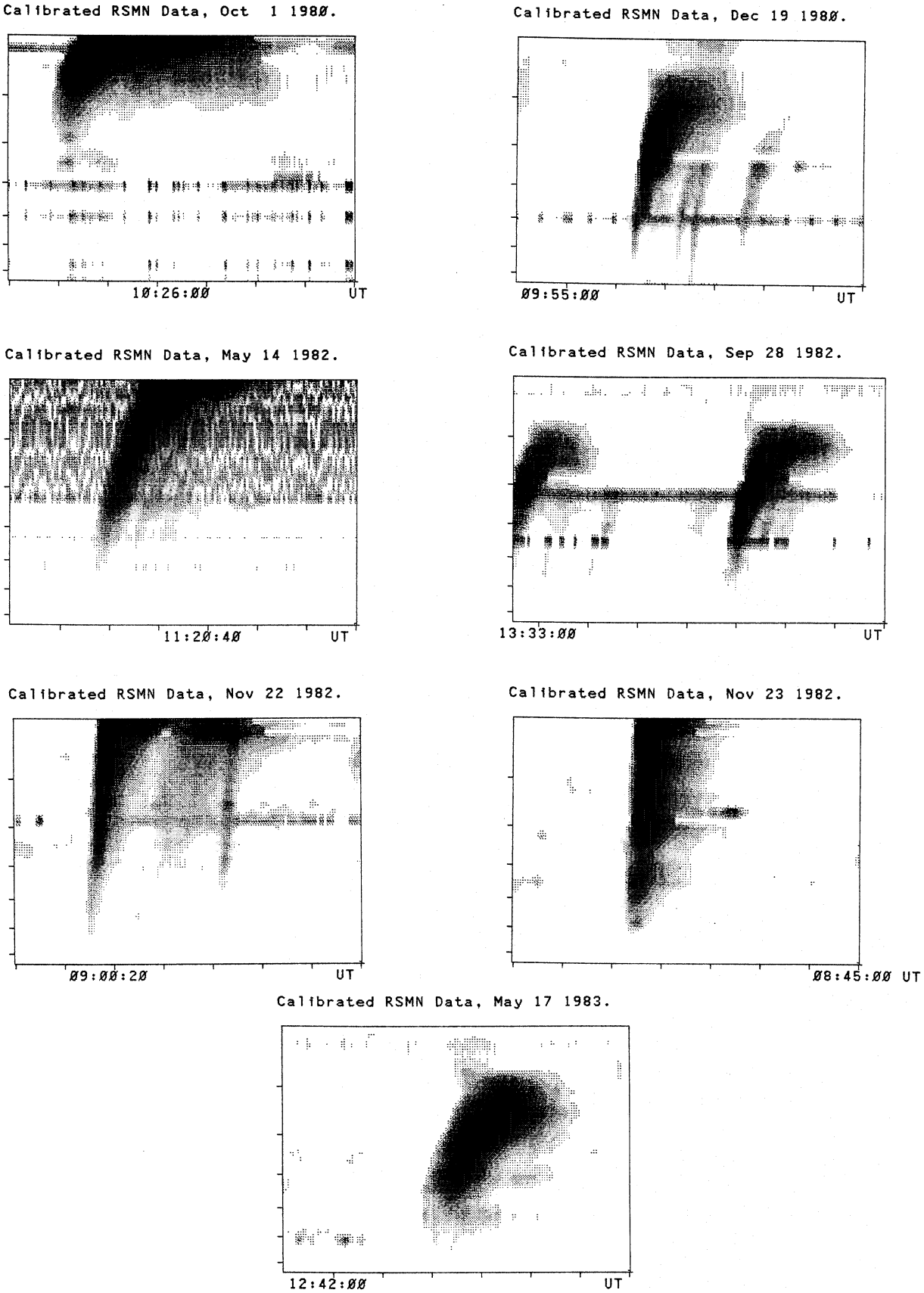

Fig. 5. Dynamic spectra of type III and J bursts observed with the Digital Multichannel Radiospectrograph of the Space Research Laboratory of the Observatory of Paris. The time marks are every 2 s and the frequency marks every 50 MHz in the range 450–200 MHz

Table 1. The isolated type III and type J bursts and the computed observable quantities

Date	Position	Time	b'	b	$\delta v/c$	v_b/c	a	h (10^3 km)
1980, October 1	N 13-E 26	10:25:56	0.330	0.622	0.54	0.48	2.5	153
1980, December 19	N 15-W 07	09:55:02	0.355	0.638	0.60	0.52	2.8	325
1982, May 14	N 03-E 28	11:20:35	0.173	0.487	0.25	0.31	1.5	180
1982, September 28	S 11-E 06	13:33:07	0.250	0.312	0.35	0.39	3.0	112
1982, November 22	N 12-W 26	09:00:15	0.279	0.550	0.42	0.42	1.35	78
1982, November 23	S 05-W 51	08:44:49	0.256	0.658	0.37	0.38	1.3	74
1983, May 17	S 12-W 61	12:42:03	0.140	0.263	0.13	0.24	1.8	158

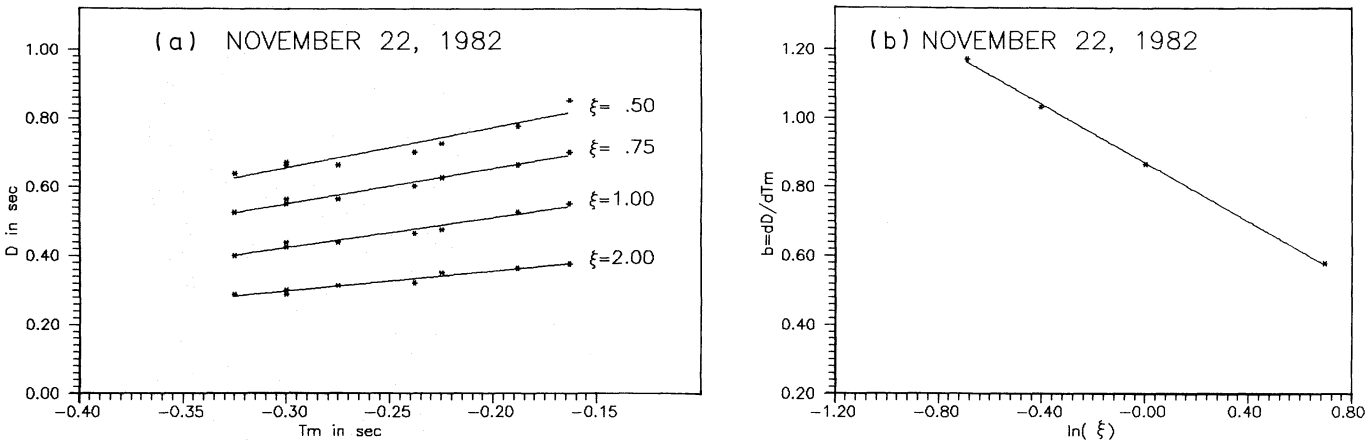

Fig. 6. **a** Half power duration as a function of the time of maximum and the parameter ξ. **b** The form factor b as a function of ln ξ for the event of November 22, 1982

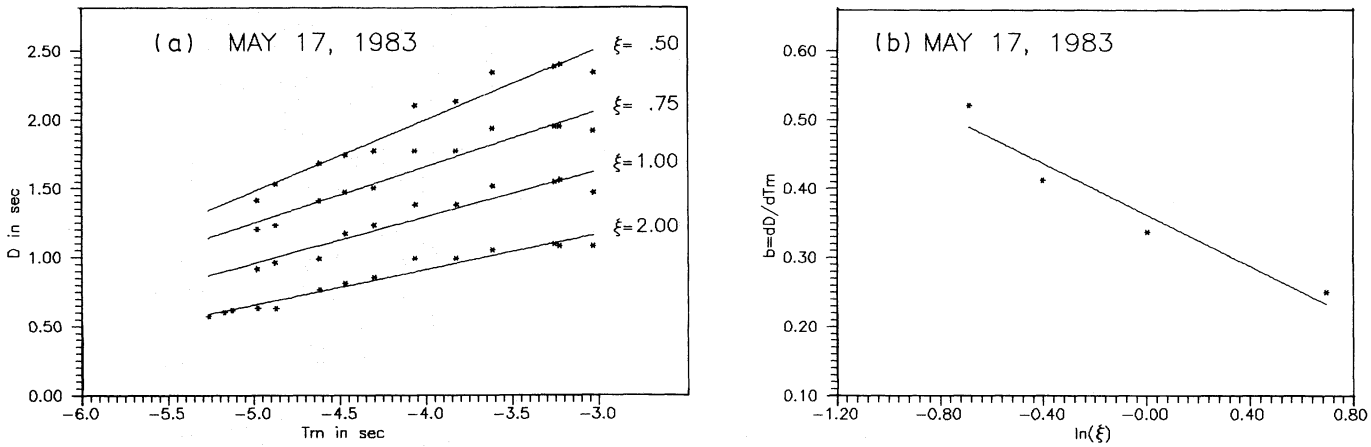

Fig. 7a and b. Same as Fig. 6 for the event of May 17, 1983

profile. A similar procedure was followed by Poquerusse (1977), however without scaling in time due to the small frequency range in his data. The results for 2 events are shown in Fig. 8, together with average theoretical profiles. The latter were also computed using the similarity property (with the same scaling factor and time shifts as the observational data), as well as the parameters determined from the observations. The agreement between the two shows that, at least in the phenomenological sense, our model describes fairly well the observational properties of the bursts.

5. Summary and conclusions

Using a simple, free-streaming model for the propagation of energetic electrons in open or closed magnetic field configurations (with very small magnetic field gradients) and the assumption of a power law dependence of the electromagnetic emission on the electron density of the beam, we computed observable quantities as a function of beam parameters. Our results are applicable in the analysis of dynamic spectra of type III and J bursts.

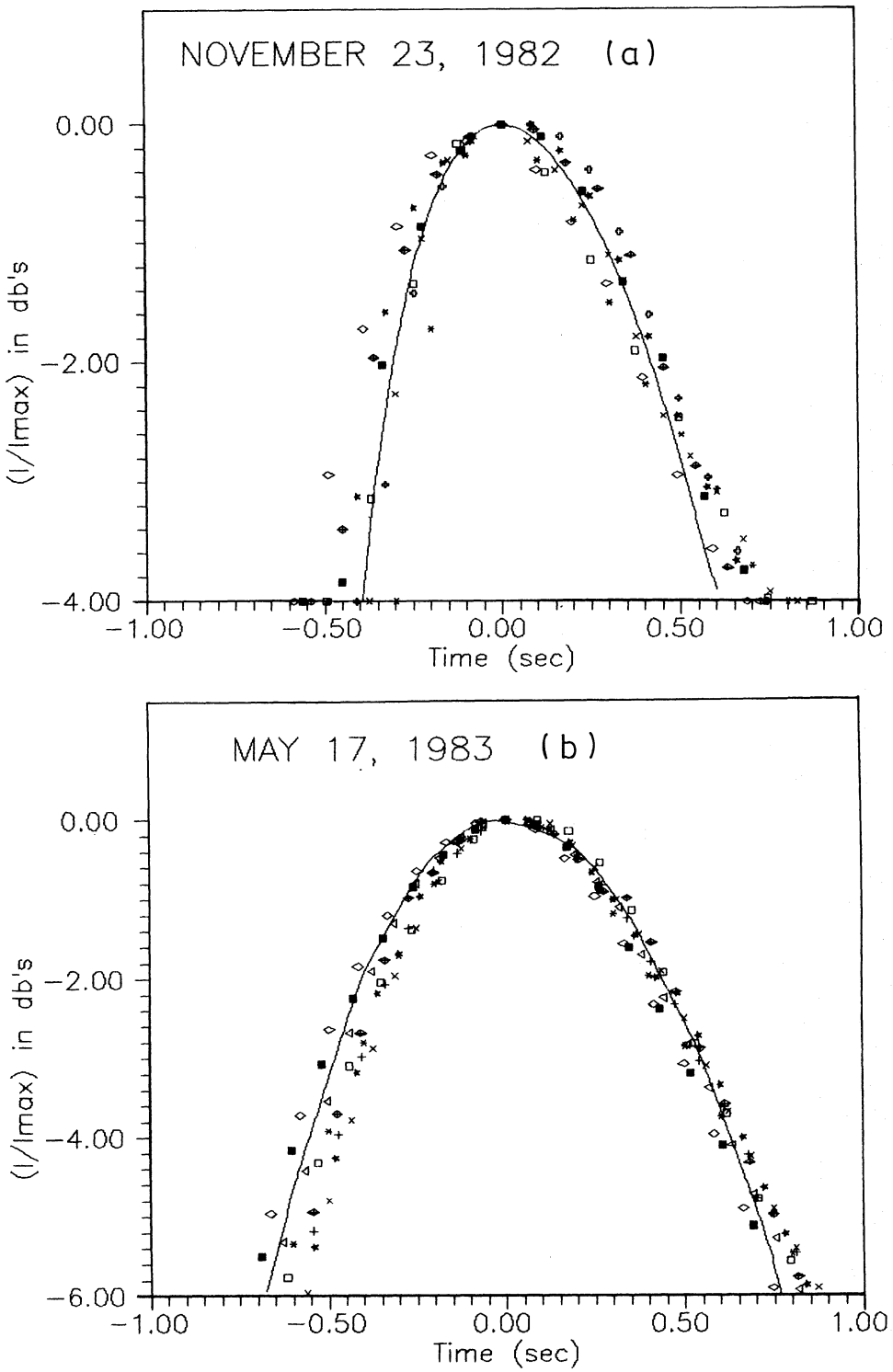

Fig. 8a and b. Superposition of intensity – time profiles at several frequencies. **a** Event of 17 May 83 12:42 UT. **b** Event of 23 Nov 82 8:44 UT. The profiles at each frequency have been normalised to the same maximum intensity and are centered to the same time of maximum; the time scales have been normalised with respect to the event duration observed at each frequency. The resulting data points are compared with a theoretical intensity-time profile (solid line). The parameters of the simulated profile are given in Table 1. The different symbols correspond to different frequencies

We showed that the initial velocity dispersion of the energetic electrons and the index of the power law relating the electron density of the beam and the flux of electromagnetic emission can be determined from measurements of the duration and the shape of observed time profiles. In addition, our numerical computations give the apparent drift velocit of the beam which, in conjunction with measurements of the frequency drift on dynamic spectra, can provide estimates of the density scale height of the ambient plasma, along the beam trajectory.

The results of the numerical simulation were applied in the analysis of seven isolated bursts observed with the Digital Multichannel Radiospectrograph of the Space Research Laboratory of the Observatory of Paris, Meudon. Furthermore, based on the results of the analysis of two "standard" type III bursts and five J bursts we were able to suggest that the emission process includes both scattering of Langmuir waves on ion acoustic waves and the polarization clouds of the ions, while the electron acceleration mechanism has to account for energies up to 100 keV.

The calculated density scale height in closed loops (corresponding to J bursts) is greater than the scale height in open loops; this implies a somewhat higher temperature within closed loops in the vicinity of active centres and/or an inclination of the field lines with respect to the vertical.

Acknowledgements. The authors are grateful to Dr. L. Vlahos for helpful comments and critical reading of the draft. Travel funds for this work have been provided in part through the bilateral scientific exchange program between France and Greece.

References

Alvarez, H., Lin, R., Bame, S.: 1975, *Solar Phys.* **44**, 485
Barrow, H., Achong, A.: 1975, *Solar Phys.* **45**, 459
Bhatnagar, P.L., Gross, E.P., Krook, M.: 1954, *Phys. Rev.* **94**, 511
Caroubalos, C., Poquerusse, M., Bougeret, J.L., Crepel, R.: 1987, *Astrophys. J.* **319**, 503
Dumas, G., Caroubalos, C., Bougeret, J.L.: 1982, *Solar Phys.* **81**, 383
Fainberg, J., Stone, R.G.: 1970, *Solar Phys.* **15**, 433
Fitzenreiter, R., Evans, L., Lin, R.: 1976, *Solar Phys.* **46**, 437
Fokker, A.D.: 1969, *Solar Phys.* **8**, 376
Goldstein, M., Smith, R., Papadopoulos, K.: 1979, *Astrophys. J.* **234**, 683
Hillaris, A., Alissandrakis, C., Vlahos, L.: 1988, *Astron. Astrophys.* **195**, 301
Ishimaru, S.: 1986, *Plasma Physics an Introduction to Statistical Physics of Charged Particles*, Benjamin Cunning, California
Lin, R.P.: 1985, *Solar Phys.* **100**, 537
Lin, R.P., Potter, D.W., Gurnet, D.A., Scarf, F.L.: 1981, *Astrophys. J.* **252**, 364
Papadopoulos, K.: 1975, *Phys. Fluids* **18**, 1769
Papadopoulos, K.: 1977, *Rev. Geophys. Space Phys.* **15**, 173
Papadopoulos, K., Freud, H.P.: 1979, *NRL Memo. Rept.* **3922**
Papadopoulos, K.: 1980, *Radio Physics of the Sun*, eds. M. Kundu, Gergely, Reidel, Dordrecht, p. 287
Poquerusse, M.: 1977, *Astron. Astrophys.* **56**, 251
Posquerusse, M., Bougeret, J.–L., Caroubalos, C.: 1984, *Astron. Astrophys.* **136**, 10
Raoult, A., Vlahos, L., Mangeney, A.: 1990, *Astron. Astrophys.* (submitted)
Ryutov, D.D., Sagdeev, R.V.: 1970, *Soviet Phys. JETP* **31**, 396
Smith, D., Davis, W.: 1975, *Solar Phys.* **41**, 439
Vlahos, L., Rowland, H.: 1984, *Astron. Astrophys.* **139**, 263
Weber, R.: 1978, *Solar Phys.* **59**, 377
Wild, J.P., McCready, L.: 1950, *Australian J. Phys.* **7**, 439
Wild, J.P.: 1970, *Proc. Astron. Soc. Australia* **1**, 365
Wild, J.P., Smerd, S.: 1972, *Ann. Rev. Astron. Astrophys.* **10**, 159
Zheleznyakov, V., Zaitsev, V.V.: 1970, *Soviet Astron.* **14**, 250